

## Design and Analysis of Partially Parallel Encoder for 16-Bit Polar Codes

**N.Chandu**

**M.Tech (VLSI Design)  
Department of ECE**

**Shree Institute of Technical Education,  
Krishnapuram, Tirupati(Rural),  
Andhra Pradesh.**

**Mrs.M.Kalpana, M.Tech**

**Assistant Professor  
Department of ECE**

**Shree Institute of Technical Education,  
Krishnapuram, Tirupati(Rural),  
Andhra Pradesh.**

### **ABSTRACT**

*Polar codes have become an important error correction codes due to their competence achieving property. Successive cancellation (SC) algorithm is considered as a good candidate for hardware design of polar decoders due to its low complexity. Although the previous fully parallel encoder is sensitive and easy to implement, it is not suitable for long polar codes because of the huge hardware complexity required. The Partial parallel encoder is intuitive and easy to implement, it is not suitable for long polar codes because of the huge hardware complexity required. The partial parallel encoder architecture that is adequate for long polar codes but increases in delay. The proposed architecture is used to avoid the faulty outputs in the propagation path of encoder circuit and delay element is added in each and every stage to get fault free output. In this brief, we analyze the encoding process in the viewpoint of very-large-scale integration implementation and simulation result shows the reduction in faulty output.*

### **I. INTRODUCTION**

Polar code is a linear block error correcting code. The code construction is based on a multiple recursive concatenation of a short kernel code which transforms the physical channel into virtual outer channels. When

the number of recursions becomes large, the virtual channels tend to either have high reliability or low reliability (in other words, they polarize), and the data bits are allocated to the most reliable channels.

Polar-coding is a capacity achieving code setting up method mainly for binary-input discrete memory much less channels. This can be done by the phenomenon of channel-polarization that every channel processes a flawlessly secure else a fully noisy channel as the code-length drives beyond over a collective channel built using a suite of N same sub channels<sup>1</sup>. 50% of power consumption can be reduced by parallel processing of two-input samples which reduces the frequency of operation by. For small or adequate polar code, fault performance by the Cyclic Redundancy Check (CRC) supported Successive Cancellation List (SCL) decoding procedure is improved than the Successive Cancellation (SC) decoding process<sup>3</sup>, which isn't appropriate for lengthy polar-codes owing to extreme hardware density. Linear block code with appropriate parameters can be used to perform block wise decoding of outer codes if there is not take into account, not necessary polar, as C 4. Path-search techniques for coding tree polar-codes are given as combined depiction of the SC, SCL, and SCS decoding algorithm. Integration of SCL and SCS, a

new decoding process called the Successive Cancellation Hybrid (SCH). A semi-parallel- encoder based partial-sum update features as accessible architecture for SC decoding of polar-codes. This module uses Static Random Access Memory (SRAM) for storing, and uses a fixed data path. This design influences a multi-level quantization structure for Limb Lengthening and Reconstruction society (LLRs), reducing the memory usage and area.

Polar-codes require tremendous code lengths to strategy the capacity of the underlying channel<sup>6</sup>. Coding theorem by Shannon’s proof for noisy channel is random coding method which is used to exhibit the presence of ability-reaching code structures without revealing any designated one<sup>7</sup>. In realistic implementations, the memory measurement and the usage of XOR-gates expand because code size increases. The polar-decoders is 8 times more than the successive cancellation decoder to increase the throughput of polar- decoding by an order of magnitude<sup>8</sup>. None of the previous works has deeply analyzed the best way to the polar-code encoding effectively, although quite a lot of trade-offs are feasible among the latency and hardware difficulty.

This design synthesized in a CMOS technology of 130nm for a parallel structure. Then again, the complex parallel structure has benefits of low latency and high throughput. The Polar Cosine Transform (PCT) algorithm used to divide the image into overlapping patches and then feature vectors are extracted from the patches. Hence, the polarization method is used in the image encryption and decryption<sup>9</sup>. Folding Transformation is a technique in which the number of butterflies in the same column is mapped into one butterfly unit. A pipelined parallel Fast Fourier Transform (FFT) architecture which has a lesser power consumption compared to serial FFT architectures. Digital Signal Processor (DSP) operations are repetitive and periodic in nature.

The life time chart specifies the life period of all variables in a single frame and the subsequent frames are computed in a periodic manner.

## II. EXISTING SYSTEM

Polar code is a new class of error correcting codes that provably achieves the capacity of the underlying channels. In addition concrete algorithms for constructing, encoding and decoding the code are all developed. Due to the channel capacity achieving property, the polar code is now considered as a major breakthrough in coding theory, and the applicability of the polar code is being investigated in many application including data storage devices. The property of efficient error correcting codes based upon the channel capacity, the code length should be at least  $2^{20}$ bits, and many literature works introduces polar codes ranging from  $2^{10}$  to  $2^{15}$  to achieve good error-correcting performances in practice. In addition, the size of a message protected by an error-correcting code in storage systems in normally 4096 bytes. Although the polar code has been regarded as being associated with low complexity, such a long polar code suffers from severe hardware complexity and long latency,. The polar code utilizes the channel polarization phenomenon that each channel approaches either a perfectly reliable or a completely noisy channel as the code length goes to infinity over a combined channel constructed with a set of N identical sub-channels. As the reliability of each sub-channel known a priori, K most reliable sub-channels are used to transmit information and the remaining sub-channels are set to predetermined values to construct a polar (N,K) code.

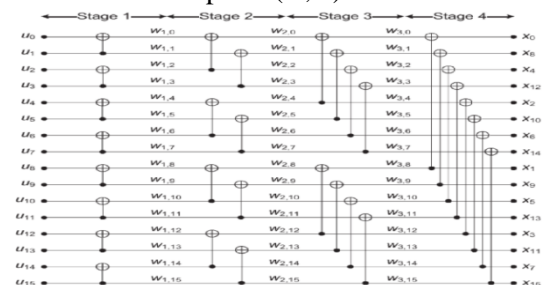


**Figure 1: Parallel architecture for encoding a 16-bit polar code.**

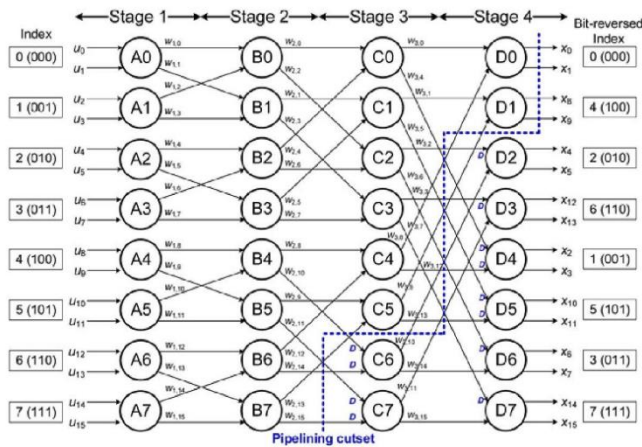


**Figure 2: DFG of 16 bit polar encoding**

The fully parallel encoder is intuitively designed based on the generator matrix, but implementing such an encoder becomes a significant burden when a long polar code is used to achieve a good error correcting performance. In Practical implementation, the memory size and the number of XOR gates increase as the code length increases.

**Disadvantages:**

1. More Hardware complexity
2. More Power dissipation
3. Not support for long polar codes

**III. PROPOSED SYSTEM**

In this section, we propose a partially parallel structure to encode long polar codes efficiently. To clearly show the proposed approach and how to transform the architecture, a 4-parallel encoding architecture for the 16-bit polar code is exemplified in depth. The fully parallel encoding architecture is first transformed to a folded form and then the lifetime analysis and register allocation are applied to the folded architecture. Lastly, the proposed parallel architecture true for long polar code is described.

**A. Folding Transformation**

The folding transformation [15], [18] is widely used to save hardware resources by time-multiplexing several

operations on a functional unit. A data flow graph (DFG) corresponding to the fully parallel encoding process for 16-bit polar codes is shown in Fig. 2, where a node represents the kernel matrix operation  $F$ , and  $w_{ij}$  denotes the  $j$ th edge at the  $i$ th stage. Note that the DFG of the fully parallel polar encoder is similar to that of the fast Fourier transform [18], [19] except that the polar encoder employs the kernel matrix instead of the butterfly operation. Given the 16-bit DFG, the 4-parallel folded architecture that processes 4 bits at a time can be realized with placing two functional units in each stage since the functional unit computes 2 bits at a time. In the folding transformation, determining a folding set, which represents the order of operations to be executed in a functional unit, is the most important design factor [15]. To construct efficient folding sets, all operations in the fully parallel encoding are first classified as separate folding sets. Since the input is in a natural order, it is reasonable to alternatively distribute the operations in the consecutive order. Thus, each stage consists of two folding sets, each of which contains only odd or even operations to be performed by a separate unit.

Considering the four-parallel input sequence in a natural order, stage 1 has two folding sets of  $\{A0, A2, A4, A6\}$  and  $\{A1, A3, A5, A7\}$ . Each folding set contains four elements, and the position of an element represents the operational order in the corresponding functional unit. Two functional units for stage 1 execute  $A0$  and  $A1$  simultaneously at the beginning and  $A2$  and  $A3$  at the next cycle, and so forth. The folding sets of stage 2 have the same order as those of stage 1, i.e.,  $\{B0, B2, B4, B6\}$  and  $\{B1, B3, B5, B7\}$ , since the four-parallel input sequence of stage 2 is equal to that of stage 1. Furthermore, to determine the folding sets of another stage  $s$ , the property that the functional unit processes a pair of inputs whose indices differ by  $2s-1$  is exploited. In the case of stage 3, two data whose indices differ by 4 are processed together, which implies that the operational distance of the corresponding data is two as the kernel functional



unit computes two data at a time. For instance,  $w_{2,0}$  and  $w_{2,4}$  that come from  $B_0$  and  $B_2$  are used as the inputs to  $C_0$ . Since both inputs should be valid to be processed in a functional unit, the operations in stage 3 are aligned to the late input data. Cyclic shifting the folding sets right by one, which can be realized by inserting a delay of one time unit, is to enable full utilization of the functional units by overlapping adjacent iterations. As a result, the folding sets of stage 3 are determined to  $\{C_6, C_0, C_2, C_4\}$  and  $\{C_7, C_1, C_3, C_5\}$ , where  $C_6$  in the current iteration is overlapped with  $A_0$  and  $B_0$  in the next iteration. In the same manner, the property that the functional unit processes a pair of inputs whose indices differ by 8 is exploited in stage 4. The folding sets of stage 4 are  $\{D_2, D_4, D_6, D_0\}$  and  $\{D_3, D_5, D_7, D_1\}$ , which are obtained by cyclic shifting the previous folding sets of stage 3 by two. Generally speaking, a stage whose index  $s$  is less than or equal to  $\log_2 P$ , where  $P$  is the level of parallelism, has the same folding sets determined by evenly interleaving the operations in the consecutive order, and another stage whose index  $s$  is larger than  $\log_2 P$  has the folding sets obtained by cyclic shifting the previous folding sets of stage  $s - 1$  right by  $s - \log_2 P$ .

Cycle	Stage2	R <sub>1</sub>	R <sub>2</sub>	R <sub>3</sub>	R <sub>4</sub>	Stage3	R <sub>5</sub>	R <sub>6</sub>	R <sub>7</sub>	R <sub>8</sub>	R <sub>9</sub>	R <sub>10</sub>	R <sub>11</sub>	R <sub>12</sub>
0	$w_{2,0}$ $w_{2,2}$ $w_{2,4}$ $w_{2,6}$					$w_{3,0}$ $w_{3,2}$ $w_{3,4}$ $w_{3,6}$								
1	$w_{2,2}$ $w_{2,4}$ $w_{2,6}$ $w_{2,8}$	$w_{2,2}$ $w_{2,4}$ $w_{2,6}$ $w_{2,8}$				$w_{3,0}$ $w_{3,2}$ $w_{3,4}$ $w_{3,6}$								
2	$w_{2,4}$ $w_{2,6}$ $w_{2,8}$ $w_{2,10}$	$w_{2,4}$ $w_{2,6}$ $w_{2,8}$ $w_{2,10}$	$w_{2,4}$ $w_{2,6}$ $w_{2,8}$ $w_{2,10}$			$w_{3,0}$ $w_{3,2}$ $w_{3,4}$ $w_{3,6}$	$w_{3,4}$ $w_{3,6}$ $w_{3,8}$ $w_{3,10}$							
3	$w_{2,6}$ $w_{2,8}$ $w_{2,10}$ $w_{2,12}$	$w_{2,6}$ $w_{2,8}$ $w_{2,10}$ $w_{2,12}$	$w_{2,6}$ $w_{2,8}$ $w_{2,10}$ $w_{2,12}$	$w_{2,6}$ $w_{2,8}$ $w_{2,10}$ $w_{2,12}$		$w_{3,0}$ $w_{3,2}$ $w_{3,4}$ $w_{3,6}$	$w_{3,2}$ $w_{3,4}$ $w_{3,6}$ $w_{3,8}$	$w_{3,2}$ $w_{3,4}$ $w_{3,6}$ $w_{3,8}$						
4		$w_{2,8}$ $w_{2,10}$ $w_{2,12}$ $w_{2,14}$	$w_{2,8}$ $w_{2,10}$ $w_{2,12}$ $w_{2,14}$	$w_{2,8}$ $w_{2,10}$ $w_{2,12}$ $w_{2,14}$	$w_{2,8}$ $w_{2,10}$ $w_{2,12}$ $w_{2,14}$	$w_{3,0}$ $w_{3,2}$ $w_{3,4}$ $w_{3,6}$	$w_{3,2}$ $w_{3,4}$ $w_{3,6}$ $w_{3,8}$	$w_{3,4}$ $w_{3,6}$ $w_{3,8}$ $w_{3,10}$	$w_{3,4}$ $w_{3,6}$ $w_{3,8}$ $w_{3,10}$					
5			$w_{2,10}$ $w_{2,12}$ $w_{2,14}$ $w_{2,16}$	$w_{2,10}$ $w_{2,12}$ $w_{2,14}$ $w_{2,16}$	$w_{2,10}$ $w_{2,12}$ $w_{2,14}$ $w_{2,16}$	$w_{3,0}$ $w_{3,2}$ $w_{3,4}$ $w_{3,6}$	$w_{3,2}$ $w_{3,4}$ $w_{3,6}$ $w_{3,8}$	$w_{3,4}$ $w_{3,6}$ $w_{3,8}$ $w_{3,10}$	$w_{3,6}$ $w_{3,8}$ $w_{3,10}$ $w_{3,12}$					
6				$w_{2,12}$ $w_{2,14}$ $w_{2,16}$ $w_{2,18}$	$w_{2,12}$ $w_{2,14}$ $w_{2,16}$ $w_{2,18}$	$w_{3,0}$ $w_{3,2}$ $w_{3,4}$ $w_{3,6}$	$w_{3,2}$ $w_{3,4}$ $w_{3,6}$ $w_{3,8}$	$w_{3,4}$ $w_{3,6}$ $w_{3,8}$ $w_{3,10}$	$w_{3,6}$ $w_{3,8}$ $w_{3,10}$ $w_{3,12}$	$w_{3,6}$ $w_{3,8}$ $w_{3,10}$ $w_{3,12}$				

Fig.3. Register allocation table for  $w_{2j}$  and  $w_{3j}$ .

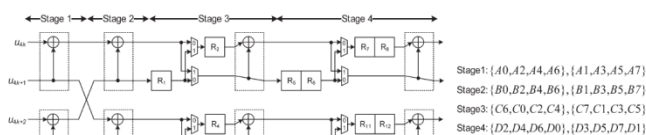


Figure 4: Proposed 4 parallel architecture of polar codes.

Now, let us consider the delay elements required in the folded architecture more precisely. When an edge  $w_{ij}$  from functional unit  $S$  to functional unit  $T$  has a delay

of  $d$ , the delay requirements for  $w_{ij}$  in the  $F$ -folded architecture can be calculated as

$$D(w_{ij}) = Fd + t - s \quad (1)$$

where  $t$  and  $s$  denote the position in the folding set corresponding to  $T$  and  $S$ , respectively. Note that (1) is a simplified delay equation [15] derived with assuming that the kernel functional unit is not pipelined. The delay requirements of the 4-folded architecture, i.e.,  $D(w_{ij})$  for  $1 \leq i \leq 3$  and  $0 \leq j \leq 15$ , are summarized in Fig. 3. For instance,  $w_{2,0}$  from  $B_0$  to  $C_0$  demands one delay since  $d = 0$ ,  $t = 1$ , and  $s = 0$ . Note that some edges indicated by circles have negative delays. For the folded architecture to be feasible, the delay requirements must be larger than or equal to zero for all the edges. Pipelining or retiming techniques can be applied to the fully parallel DFG in order to ensure that its folded hardware has nonnegative delays. Every edge with a negative delay should be compensated by inserting at least one delay element to make the value of (1) not negative. We have to make sure that the two inputs of an operation pass through the same number of delay elements from the starting points. If they are different, additional delay elements are inserted to make the paths have the same delay elements. In Fig. 3, for example, four edges with zero delays are specially marked with negative zeros since additional delays are necessary due to the mismatch of the number of delay elements. The DFG is pipelined by inserting delay elements, as shown in Fig. 2, where the dashed line indicates the pipeline cut set associated with 12 delay elements. The delay requirements of the pipelined DFG  $Dr(w_{ij})$  are recalculated based on (1) and shown at the bottom of Fig. 3. As a result, 8 functional units and 48 delay elements in total are enough to implement the 4-parallel 4-folded encoding architecture based on the folding sets.

## B. Lifetime Analysis and Register Allocation

Although a folded architecture for 16-bit polar encoding is presented in the previous section, there is room for minimizing the number of delay elements.

The lifetime analysis [16] is employed to find the minimum number of delay elements required in implementing the folded architecture. The lifetime of every variable is graphically represented in the linear lifetime chart illustrated in Fig. 4. Since all the edges starting from stage 1 demand no delay elements, only  $w_{2j}$  and  $w_{3j}$  are presented in Fig. 4. For instance,  $w_{3,0}$  is alive for two cycles as it is produced at cycle 1 and consumed at cycle 3. The number of variables alive in each cycle is presented at the right side of the chart. Note that the number of live variables at the fourth or later clock cycles takes into account the next iteration overlapped with the current iteration. Consequently, the maximum number of live variables is 12, which means that the folded architecture can be implemented with 12 delay elements instead of 48.

Once the minimum number of delay elements has been determined, each variable is allocated to a register. For the above example, the register allocation is tabularized in Fig. 5. In the register allocation table [17], all the 12 registers are shown at the first row, and every row describes how the registers are allocated at the corresponding cycle. With taking into account the 4-parallel processing, variables are carefully allocated to registers in a forward manner. In Fig. 5, an arrow dictates that a variable stored in a register is migrated to another register, and a circle indicates that the variable is consumed at the cycle. For example,  $w_{2,0}$  and  $w_{2,4}$  are consumed in a functional unit to execute operation C0 that generates  $w_{3,0}$  and  $w_{3,4}$ . At the same time,  $w_{2,1}$  and  $w_{2,5}$  are consumed in another functional unit to execute operation C1 that produces  $w_{3,1}$  and  $w_{3,5}$ . The migration of the other variables can be traced by following the register allocation table.

Finally, the resulting 4-parallel pipelined structure proposed to encode the 16-bit polar code is illustrated in Fig. 6, which consists of 8 functional units and 12 delay elements. A pair of two functional units takes in charge of one stage, and the delay elements are to store variables according to the register allocation table. The hardware structures for stages 1 and 2 can

be straightforwardly realized as no delay elements are necessary in those stages, whereas for stages 3 and 4, several multiplexers are placed in front of some functional units to configure the inputs of the functional units. The proposed architecture continuously processes four samples per cycle according to the folding sets and the register allocation table. Note that the proposed encoder takes a pair of inputs in a natural order and generates a pair of outputs in a bit-reversed order, as shown in Fig. 2. As the functional unit in the proposed architecture processes a pair of 2 bits at a time, the proposed architecture maintains the consecutive order at the input side and the bit-reversed order at the output side if a pair of consecutive bits is regarded as a single entity.

In the proposed system of 4 parallel architecture of polar code to be re-modified and to implement 8-parallel architecture of polar code, and finally show the same power consumption, and the report of area, delay and logic sizes.

### Advantages

1. Less Hardware complexity
2. More power consumption
3. Support for long polar codes

### IV. ANALYSIS AND COMPARISON

In the proposed architecture, the number of functional units required in the implementation depends on the code length  $N$  and the level of parallelism  $P$ . Since a functional unit representing the kernel matrix  $F$  processes two bits at a time, each stage necessitates  $\lceil P/2 \rceil$  functional units and the whole structure requires  $\lceil P/2 \rceil \log_2 N$  functional units in total.

TABLE I  
COMPARISON OF POLAR  $(N, K)$  ENCODERS  
WITH VARIOUS PARALLELISM

Parallelism	XOR gates	Delay elements	Throughput
1	$\log_2 N$	$N-1$	1 bit/cycle
2	$\log_2 N$	$N-2$	2 bits/cycle
$P$	$\lceil P/2 \rceil \log_2 N$	$N-P$	$P$ bits/cycle
$N$	$(N/2) \log_2 N$	0	$N$ bits/cycle

TABLE II  
SYNTHESIS RESULTS OF POLAR (8192, K) ENCODERS

Parallelism	32	128	512	2048	8192 <sup>(3)</sup>
Critical-Path Delay	2.74 ns	2.81 ns	2.89 ns	2.97 ns	3.06 ns
Latency (Clock cycles)	256	64	16	4	1
Throughput <sup>(4)</sup>	11.67 Gbps	45.55 Gbps	177.1 Gbps	689.5 Gbps	2.677 Tbps
Gate Count <sup>(5)</sup>	96626	104236	129449	198907	353141
(Logic/Register)	(377092456)	(1187592411)	(3703792412)	(10662392284)	(26098392158)
[B] / [C]	0.27	0.30	0.37	0.56	1.00
[A] / [B] (Mbps/Gate count)	0.12	0.43	1.36	3.46	7.58

TABLE III  
GATE COUNTS OF POLAR (N, K) ENCODERS

Code length	1024		2048		4196		8192		16384	
	[1]	Proposed <sup>a</sup>	[1]	Proposed <sup>a</sup>	[1]	Proposed <sup>a</sup>	[1]	Proposed <sup>a</sup>	[1]	Proposed <sup>a</sup>
Logic	13872	1486 (10.7%)	30812	1651 (5.4%)	67692	1813 (2.7%)	158848	2127 (1.3%)	371776	2490 (0.7%)
Register	7211	7283 (101.0%)	16512	16661(100.9%)	33000	33165(100.5%)	66122	66337 (100.3%)	132812	133121(100.2%)
Total	21083	8769 (41.6%)	47324	18312 (38.7%)	100692	34978 (34.7%)	224970	68464 (30.4%)	504588	135611(26.9%)

<sup>a</sup>The proposed partially parallel encoder is design with a parallelism of 32.

Moreover, the minimal number of delay elements required in the proposed architecture is  $N - P$ , as explained below. The stages whose indices  $s$  are larger than  $\log_2 P$  require  $P$  delay blocks of length  $2s - \log_2 P - 1$ , whereas the other stages can be implemented with no delay elements. In other words, the total number of delay elements is

$$\sum_{s=\log_2 P+1}^{\log_2 N} P(2^{s-\log_2 P}-1) = P(1 + 2 + \dots + 2^{\log_2 N - \log_2 P - 1}) = P(2^{\log_2 N - \log_2 P} - 1) = N - P. \quad (2)$$

Given the hardware resources, the proposed partially parallel architecture can encode  $P$  bits per cycle. To sum up, Table I shows how the hardware complexity and the throughput are dependent on the level of parallelism. Furthermore, Table II demonstrates the proposed (8192, K) encoder architecture synthesized in a 130-nm CMOS technology for various parallelism. As the level of parallelism increases, the hardware complexity measured in terms of the gate count is significantly deteriorated due to the complex logic part, whereas the register part in all encoder architectures maintains similar complexity if we take into account a  $P$ -bit input buffer needed to hold the data to be read from the memory. On the other hand, the higher parallel architecture has advantages of small latency and high encoding throughput. Therefore, the relationship shown in Table II can be applied to derive the most efficient partially parallel encoder architecture for a given requirement. The throughput

per gate is proportional to the level of parallelism as the complexity of the register part is almost independent of the parallelism. Moreover, Table III shows how much the partially parallel encoders save the hardware complexity compared with the fully parallel architecture [1] for various code lengths. For fair comparison, all the encoders designed for the code lengths ranging from 210 to 214 are constrained by a working frequency of 200 MHz to assure a decoding performance over 6.4 Gb/s even for the 32-parallel architecture. Note that the percentage in the parenthesis indicates the ratio of the proposed encoder to the fully parallel encoder. Compared with the fully parallel encoder, the proposed encoder saves the hardware by up to 73%.

## V. RESULTS

The Number of Slices, Number of Slice Flip Flops, Number of 4 input LUTs, Number of bonded IOBs, Number of GCLKs used is 63, 88, 56,66,1 respectively for the proposed system.

Logic Utilization	Device Utilization Summary (estimated values)			Utilization
	Used	Available		
Number of Slices	63	4656	1%	
Number of Slice Flip Flops	88	9312	0%	
Number of 4 input LUTs	56	9312	0%	
Number of bonded IOBs	66	232	28%	
Number of GCLKs	1	24	4%	

FIGURE 5: Device utilization summary of Proposed system.

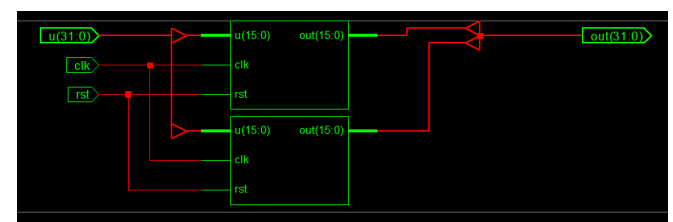


FIGURE 6: RTL Schematic of proposed system.

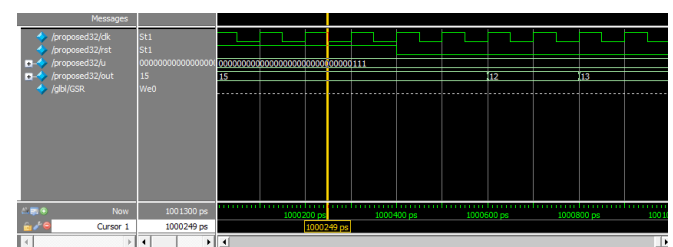


FIGURE 7: Output waveforms of proposed system.

**Maximum combinational path delay: 7.337ns**

## VI. CONCLUSION

This paper has presented a new partially parallel encoder architecture developed for long polar codes. Many optimization techniques have been applied to derive the proposed architecture. Experimental results show that the proposed architecture can save the hardware by up to 73% compared with that of the fully parallel architecture. Finally, the relationship between the hardware complexity and the throughputs is analyzed to select the most suitable architecture for a given application. Therefore, the proposed architecture provides a practical solution for encoding a long polar code.

## REFERENCES

- [1] E. Arikan, "Channel polarization: A method for constructing capacity achieving codes for symmetric binary-input memoryless channels," *IEEE Trans. Inf. Theory*, vol. 55, no. 7, pp. 3051–3073, Jul. 2009.
- [2] R. Mori and T. Tanaka, "Performance of polar codes with the construction using density evolution," *IEEE Commun. Lett.*, vol. 13, no. 7, pp. 519–521, Jul. 2009.
- [3] S. B. Korada, E. Sasoglu, and R. Urbanke, "Polar codes: Characterization of exponent, bounds, constructions," *IEEE Trans. Inf. Theory*, vol. 56, no. 12, pp. 6253–6264, Dec. 2010.
- [4] I. Tal and A. Vardy, "List decoding of polar codes," in *Proc. IEEE ISIT*, 2011, pp. 1–5.
- [5] K. Chen, K. Niu, and J. Lin, "Improved successive cancellation decoding of polar codes," *IEEE Trans. Commun.*, vol. 61, no. 8, pp. 3100–3107, Aug. 2013.
- [6] G. Sarkis and W. J. Gross, "Polar codes for data storage applications," in *Proc. ICNC*, 2013, pp. 840–844.
- [7] G. Sarkis, P. Giard, A. Vardy, C. Thibeault, and W. J. Gross, "Fast polar decoders: Algorithm and implementation," *IEEE J. Sel. Areas Commun.*, vol. 32, no. 5, pp. 946–957, May 2014.
- [8] G. Berhault, C. Leroux, C. Jégo, and D. Dallet, "Partial sums generation architecture for successive cancellation decoding of polar codes," in *Proc. IEEE Workshop SiPS*, Oct. 2013, pp. 407–412.
- [9] B. Yuan and K. K. Parhi, "Low-latency successive-cancellation polar decoder architectures using 2-bit decoding," *IEEE Trans. Circuits Syst. I, Reg. Papers*, vol. 61, no. 4, pp. 1241–1254, Apr. 2014.
- [10] C. Leroux, A. J. Raymond, G. Sarkis, and W. J. Gross, "A semi-parallel successive-cancellation decoder for polar codes," *IEEE Trans. Signal Process.*, vol. 61, no. 2, pp. 289–299, Jan. 2013.
- [11] A. J. Raymond and W. J. Gross, "Scalable successive-cancellation hardware decoder for polar codes," in *Proc. IEEE GlobalSIP*, Dec. 2013, pp. 1282–1285.
- [12] U. U. Fayyaz and J. R. Barry, "Low-complexity soft-output decoding of polar codes," *IEEE J. Sel. Areas Commun.*, vol. 32, no. 5, pp. 958–966, May 2014.
- [13] B. Yuan and K. K. Parhi, "Low-latency successive-cancellation list decoders for polar codes with multibit decision," *IEEE Trans. Very Large Scale Integr. (VLSI) Syst.*, DOI: 10.1109/TVLSI.2014.2359793, to be published.
- [14] C. Zhang and K. K. Parhi, "Latency analysis and architecture design of simplified SC polar decoders," *IEEE Trans. Circuits Syst. II, Exp. Briefs*, vol. 61, no. 2, pp. 115–119, Feb. 2014.





[15] K. K. Parhi, VLSI Digital Signal Processing Systems: Design and Implementation. Hoboken, NJ, USA: Wiley, 1999.

[16] K. K. Parhi, "Calculation of minimum number of registers in arbitrary life time chart," IEEE Trans. Circuits Syst. II, Analog Digit. Signal Process., vol. 41, no. 6, pp. 434–436, Jun. 1995.

#### **AUTHOR PROFILE**

**Mr.N.Chandu, P.G.Scholar**, Department of ECE, Shree Institute of Technical Education, Tirupati, A.P. India. He has Received his B.Tech Degree in (ECE) from Shree institute of technical education, Tirupati in 2013. Currently He is Doing M.Tech (VLSI) in Shree Institute of technical education, Tirupati. His General Areas of Interest are Low Power VLSI, Digital IC Design, Signal processing, Image processing.

**Mrs. M. Kalpana, M.Tech, [DECS]. Assistant Professor,**

She received his Master of Technology degree from JNTUA. Currently working as Assistant Professor in ECE department of SHREE Institute of Technical Education, affiliated to JNTUA, Tirupati, A.P. India. She has 5 years teaching experience in the stream of engineering education. She has 2 Published in International Journals. Her research areas are Signal processing, image processing and communications systems.